To Study the effect of nuclear potential parameters on fusion cross-section of ^{7}Li with ^{64}Ni

A Thesis submitted in partial fulfilment of the requirements for the award of the degree of

Master of Science

In

Physics

Submitted by

Hitakshi

Roll No. 301804006

Under the supervision of

Dr. Sunil Devi

Assistant professor

School of Physics and Material Science (SPMS)

Thapar Institute of Engineering and Technology, Patiala

School of Physics and Material Science (SPMS)

Thapar Institute of Engineering and Technology, Patiala

Patiala-147004, INDIA

Declaration

I hereby declare that the dissertation entitled "To study the effect of nuclear potential on fusion cross-section of ^{7}Li with ^{64}Ni" is an authentic record of my work carried out as requirement for the award of the degree of Master of Science at Thapar Institute of Engineering and Technology, Patiala under the supervision of Dr. Sunil Devi, Assistant Professor, School of Physics and Material Science, Thapar Institute of Engineering and Technology, Patiala. No part of the matter embodied in this dissertation has been submitted to any other university or institute for the award of any degree.

June 20, 2020

(Hitakshi)

301804006

It is certified that the above statement made by the student is correct to the best of my knowledge and belief.

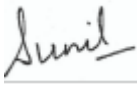

Dr. Sunil Devi

Supervisor

(Assistant Professor)

ACKNOWLEDGEMENT

This thesis becomes a reality with the kind support and help of many individuals. I would like to express my sincere thanks to all of them.

Foremost, I want to thank God Almighty for the strength and wisdom He bestowed upon me, the peace of mind and good health in order to finish my thesis.

Secondly, I would like to express my deepest thanks to my supervisor Dr. Sunil Devi for her constant guidance throughout the thesis work. This thesis work would not have been possible without her timely suggestions, her support and providing necessary information regarding my work despite of her busy schedule. I am grateful for the experience and diverse opportunity I was given while working with her.

Lastly, I would like to express my gratitude towards my family for the encouragement which helped me in completion of this thesis. My thanks and appreciation also goes to my friends and people who have willingly helped me out with their abilities.

Hitakshi

LIST OF FIGURES

Chapter 1

Chapter 2

Chapter 3

Figure 18. Variation in fusion cross-section by varying radius parameter.
Figure 19. Variation in fusion cross-section in case of deformed and inert nuclei.

Content

Abstract

- The aim of this work is to scout or explore the dependence of the fusion cross-sections on various parameters such as depth of the potential, radius and the diffusion parameter. The effect of these parameters is explored at above and below the coulomb barrier by taking loosely bound nuclei ^{7}Li as projectile and isotope of nickel that is ^{64}Ni which is a stable mass target.

  The CCFULL program is used to determine the fusion cross-section and mean angular momentum of the compound nucleus, taking into account the no-Coriolis approximations to reduce the dimensions of the coupled channel calculations. The program input parameters are given to the computer code CCFULL and the test shows the fusion cross-section for the ^{7}Li + ^{64}Ni reaction. In the first case, the projectile and the target nuclei are assumed to be spherical and measure the fusion cross-section in the absence of channel coupling. In the next case, the target is assumed to be deformed which effect the fusion cross-section. Any variation in the above three parameters affect the barrier height, the shape and depth of the potential pocket which effect the fusion cross-section of ^{7}Li + ^{64}Ni reaction.

Chapter 1

1. ***Introduction***

Nuclear reaction is a process or a reaction in which two or more than two nuclei collide with each other to give the products different from the reactants. Nuclear reactions are useful as they give us information about the excited energy levels of the nuclei. A nuclear reaction is in the form of

$$a + A = b + B$$

where a is the incoming projectile nucleus and A is the target nucleus r. b is the outgoing projectile and B is the daughter nucleus. The above nuclear reaction may also be represented as

$$A\ (a, b)\ B$$

Examples of nuclear reaction

α decay $^{238}U \rightarrow {}^{234}Th + {}^{4}He$

β decay $^{131}I \rightarrow {}^{131}Xe + {}^{0}e_{1}$

γ decay $^{234}Th^{*} \rightarrow {}^{234}Th + \gamma$

In the lab the first nuclear reaction performed was

$$_{7}N^{14}\ (\alpha, p)\ _{8}O^{17}$$

Different types of nuclear reactions

i. **Scattering:** The incoming projectile and outgoing projectile are the same in the scattering process. The scattering is said to be elastic or inelastic depending on the target. The target may be left in the ground state or excited state.

ii. **Elastic scattering:** The collision between two nucleon particles result in the elastic scattering when projectiles are scattered by the localized force field or there is no loss of kinetic energy or they are lost to the elastic channel by various

direct or indirect processes but there may be change in the direction.

$$a + A \rightarrow a + A$$

where a and A on the R.H.S are the incident projectile and the target nucleus respectively. a and A on the L.H.S are the outgoing projectile and the daughter nucleus. In this process the daughter nucleus has been left in the ground state.

iii. **Inelastic scattering:** The incoming and outgoing particles in the inelastic scattering are:

$$a + A \rightarrow a + A^*$$

where, A^* is the daughter nucleus in the excited state. In inelastic scattering the final kinetic energy will be less than the initial kinetic energy

iv. **Pick up reactions:** The projectile picks up nucleons from the target nucleus in this type of nuclear reactions.

v. **Stripping reactions:** In this type of nuclear reaction, the projectile loses nucleons such that the target nucleus absorbs part of the projectile.

All the above reactions are different type of nuclear reactions. In peripheral collision, during brief period of contact between the colliding particles direct reactions most commonly occur. Direct reactions are to be contrasted from the compound nuclear reactions. If the kinetic energy of the projectile 30 MeV, then formation of compound nucleus takes place with mass number and the charge as the sum of the charges and masses of the projectile and target nucleus. During the process of formation of the compound nucleus, the nuclei which combine to form compound nucleus will lose their identity. If the compound nucleus is formed in the excited state it decays into product particle. The decay process does not depend on the mode of

formation of the compound nucleus. The life span of the compound nucleus is about 10^{-16} s and a compound nucleus can decay into different number of modes.

1.1 Heavy-ion reactions

In heavy ion reactions the wavelength of projectile is smaller than the nuclear dimensions, and collisions can be described classically or semi-classically. There is transfer of large amounts of energy, angular momentum and nuclear material and if the collision leads to fusion the product mass will be much different from the mass of the original particles.

***Main types of heavy ion reactions*:**

The figure 1 below shows the heavy ion reaction mechanism on the basis of impact parameter. The impact parameter is the perpendicular offset of the trajectory of the incoming particle and the outgoing particle emerges at some angle.

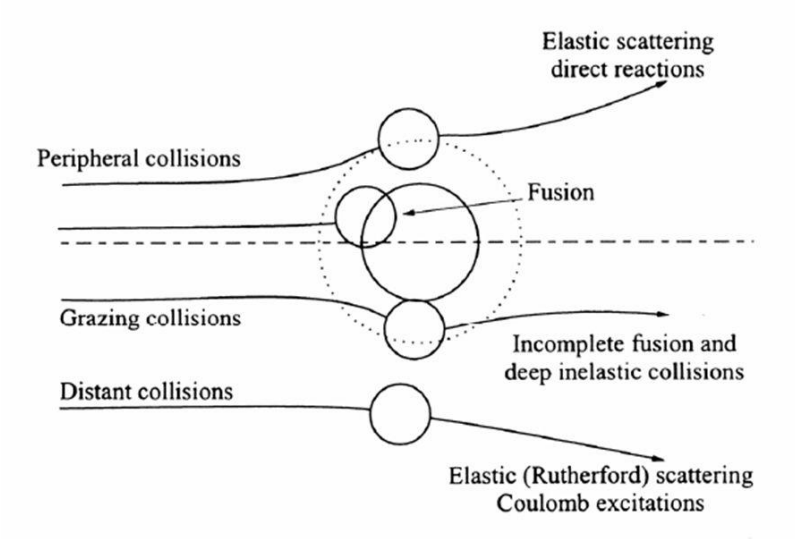

Figure 1. Diagram representation of heavy ion reaction mechanism. [Ref- Elastic scattering (Hans-Jürgen Wollersheim)]

i. *Elastic scattering and direct reactions*: Coulomb force becomes significant at low and moderate energies and plays a crucial role in

determining the heavy ion collisions. In heavy ion collision coulomb repulsion effect the trajectory near the target nucleus. When the projectile is with large impact parameter, the trajectory misses the target nucleus and the particle is scattered by the coulomb field. These collisions are called distant collisions which results in elastic scattering. Coulomb excitation takes place when the projectile passes close to the target nucleus due to strong impulse which leads to the significant amount of inelastic scattering.

During direct nuclear reactions the projectile grazes the target nucleus and the particle scatter elastically. This type of collision when the projectile just reaches the target and direct reactions takes place are called peripheral collisions. The angular distribution of the outgoing particle is of bell-shape. If θ_g corresponds to the grazing angle, then for $\theta < \theta_g$, the reaction probability got reduced as the nuclear surfaces do not approach closely. For $\theta > \theta_g$ the fusion reaction becomes predominate due to greater overlapping of nuclei during collision. The smaller angle gives the large impact parameter.

ii. *Fusion*: If the projectile collides with the target nucleus with small impact parameter, the interaction takes place inside the radius of the target nucleus which results in more complex reactions leading to the fusion. During fusion of heavy ion, formation of new nuclei takes place when the large amount of energy and momentum is transfer to the target nucleus. For example

$^{40}Ca_{20} + {}^{90}Zr_{50} \rightarrow {}^{130}Nd_{70}$

In the above reaction, two heavy ions Ca and Zr fuses to produce the compound nucleus Nd, which is proton rich, therefore when two heavy ion fuses, the compound nucleus formed is proton rich and is not much heavier than the projectile or target. Moreover, the

compound nucleus has excitation energy due to which it evaporate more neutrons and become more proton rich, and move away from the stability line. If the projectile fuses with the target nucleus with the high momentum, then compound nucleus formed will be with very high momentum.

iii. *Deep inelastic reactions and limits to fusion*: In deep inelastic collisions the interacting nuclei stay in contact for long time and during this time the combined system rotates before separation. When the collision between the nuclei results in the orbital angular momentum which exceeds the critical value of the orbital angular momentum (L_c), then combined system splits into two fragments. As the nuclei approach each other, the kinetic energy gets reduced due to conversion of kinetic energy into coulomb potential energy. The period of contact is long, therefore there is dissipation of kinetic energy into internal excitation in the form of heat. This conversion of kinetic energy into internal excitation takes place around the region of contact through nucleon-nucleon collision and mass exchange. There is exchange of particles in both the direction of the sticking nuclei. As the angular momentum is too high of the sticking nuclei, the fragments separate with a certain amount of kinetic energy and fly apart. As they repel each other mutual coulomb potential energy adds radial kinetic energy to each fragment. Nucleon transfer takes place in both direction during contact and the masses and charges of the product is not much different from those of the reactants. The time of contact is short, therefore the interaction is forward focused. Relatively high energy loss from the kinetic energy to the internal degree of freedom distinguishes the direct inelastic collisions from the quasi-elastic scattering.

Direct inelastic collisions occur when orbital angular momentum l, lies between the critical angular momentum l_c, and grazing angular momentum l_g. Quasi elastic scattering takes place when $l>l_g$ and fusion process dominates when $l<l_c$. For the path close to the l_g, coulomb excitations dominate. For large values of l and small interaction time, kinetic energy loss increases as the reaction time increases. Through exchange of nucleons kinetic energy loss into internal energy takes place and hence this loss can be used to measure the interaction time. The figure 2 given below illustrates the range of heavy-ion nuclear reaction mechanism as a function of angular momentum.

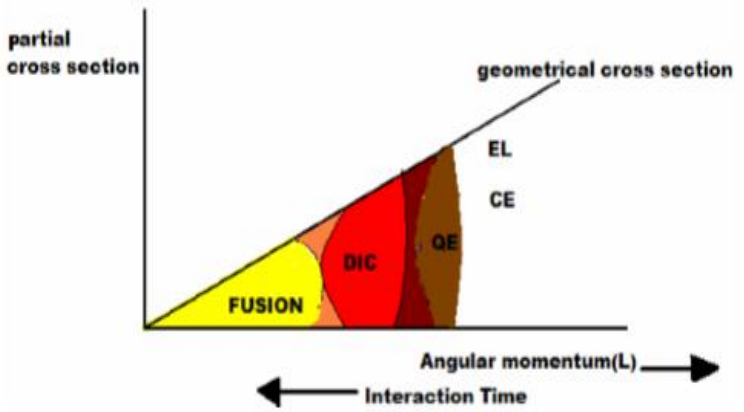

figure 2 probability of heavy-ion reaction mechanism as a function of orbital angular momentum. Below l_c fusion process predominates. In between l_c and l_g direct inelastic collisions (DIC) takes place and direct or quasi elastic collisions takes place when angular momentum l exceeds l_g.

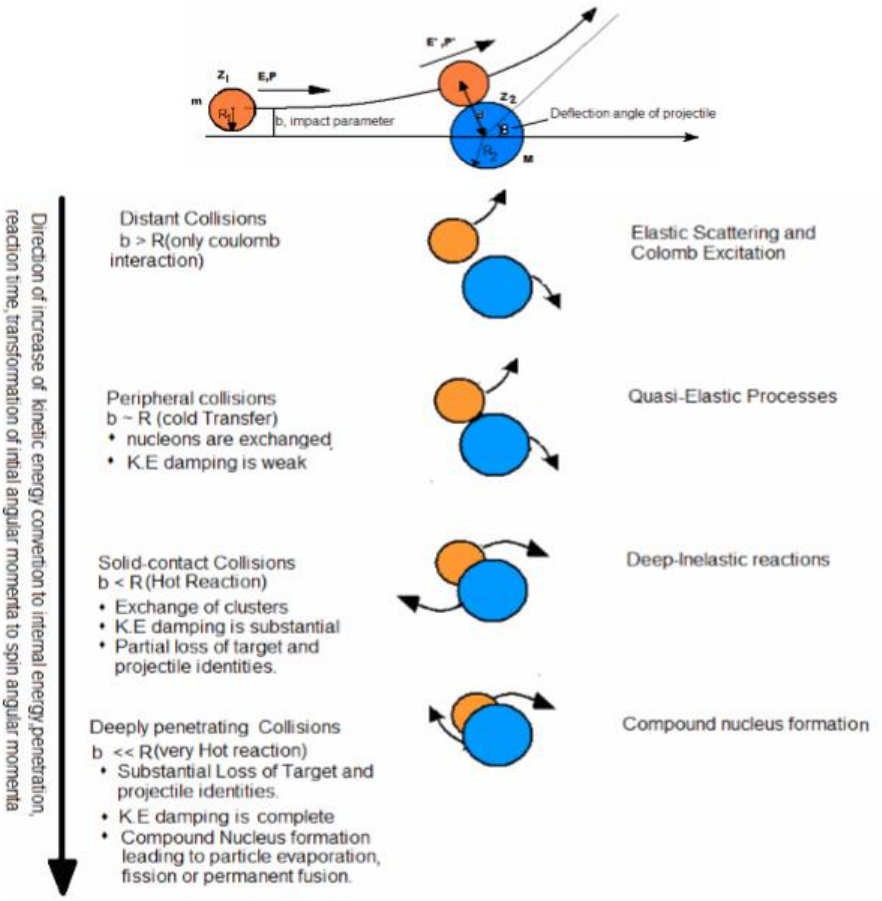

Figure 3 classical representation of grazing trajectory of the projectile and different ways of heavy ion reactions. (modified and redrawn from [4]).

Factors affecting the reaction mechanism are:

- The mass of the projectile.
- The kinetic energy of the projectile.
- The angular momentum and impact parameter of the projectile.
- The Q values of both the projectile and the target.
- As shown in figure 2 the reaction time becomes longest for the fusion in which the compound nucleus lives long to randomize completely.

In general, the fusion reaction is the one in which two light nuclei with Z<20 combine together to form a heavier nucleus with release of large amount of energy. This energy arises from the binding energy of the reactants.

Quantum tunnelling also termed as tunnelling is a phenomenon in which the nuclear particle of one side travels to the other side. Suppose the energy incident is not large and the system chosen is somehow heavy, then the reaction is driven by quantum tunnelling through the coulomb barrier. The term coulomb barrier is similar to the energy barrier in which two nuclei need to overcome this barrier for a nuclear reaction to occur.

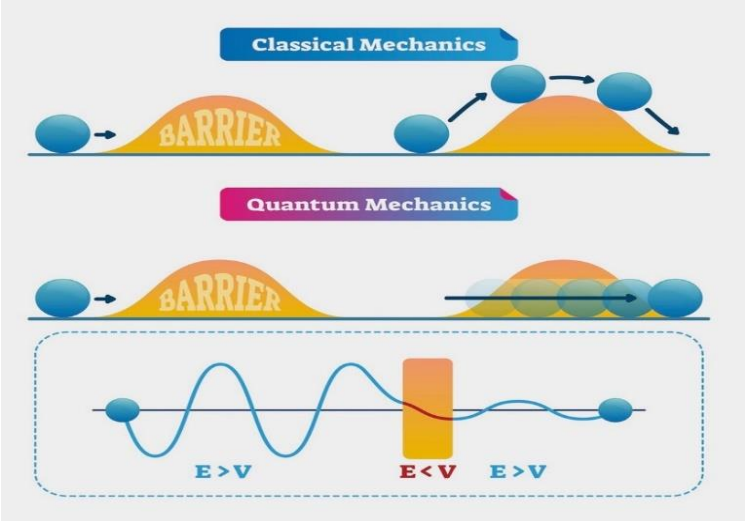

figure 4. Classical and quantum tunnelling through the barrier.[wikepedia]

According to Robert Sang " If you lean on a wall, that wall pushes back in force so that you don't go through it." He further adds that when you go down to the microscopic level this behave quite

differently because of the law of physics change from classical to quantum. As a consequence of this “ a particle in the quantum world can pass through the wall.

There are many reaction mechanisms possible when two nuclei interact with each other. In order to comprehend the Couple Channel equations, let us consider the two nuclei X and Y as bunch of individual nucleons. Then fold the nucleon-nucleon interactions with the dispersion or distribution of nucleon inside each of the pair of the nuclei to estimate the interaction between the two. As a consequence of this, the dislocation of nucleons within the two nuclei as a function of distance between them take place. In this way numerous arrangements may be feasible. Relying on the energy of the interactions, it is quite believed that many halfway excited states, such as single particle excited states are produced during the collision process, or one or two nucleons shifted between the nuclei, or nuclei join at the closest approach, devising in a compound nucleus. In this case relative motion will couple to the changes in the state. These rearrangements are termed as channels, and there may be more than one internal re-arrangement possible from incident of X on Y.

The program CCFULL solves the couple channel equations in which CCFULL directly integrates coupled second order differential equations to culminate fusion cross-sections and angular momenta of the composite system. It depends on the supposition that the fusion phenomenon is ruled by quantum tunnelling through the coulomb barrier as low energy heavy-ion reactions are governed by the quantum tunnelling through the barrier.

The program CCFULL comprises the couplings to full order but the size of coupled channel equations is too large and the program makes

use of no-Coriolis approximation which is sometimes referred to as rotating frame approximation which in turn reduces the couple channels to be solved [1,2]. It is a sudden tunnelling approximation which includes coulomb excitations and uses the arriving wave boundary pathology inside the coulomb barrier.

1.2 ***Cross-sections***

When collision of particles takes place, cross-section measures the possibility of the reaction to take place at that particular time. During the interaction of two particles or particle-particle collisions between the atoms or molecules, their cross-section is oblique, and they meet during their relative motion in order to scatter from each other. The scattering can be elastic and inelastic scattering. Different final states have its own probability. We can roughly estimate cross section from the classical and quantum mechanical approach.

Classical estimation

When the cross-section is dependent on some variable, then this type of cross section is named as differential cross-section. When the cross-section is integrated over all the angles, it is called as total cross-section. The total cross-section is separated into two parts elastic scattering cross-section σ_{sc} and reaction cross-section σ_r. Thus,

$$\sigma_t = \sigma_{sc} + \sigma_r$$

If the nuclei approach each other and the distance between their centers is less than the interaction radius R, then a nuclear reaction take place. And if the distance between their centers is greater than the interaction radius, i.e. $r > R$, no reaction takes place. The interaction radius depends upon the interacting nuclei. The figure 5 given below represents the interaction radii R, as the sum $R_1 + R_2$ of the effective radii of the two nuclei.

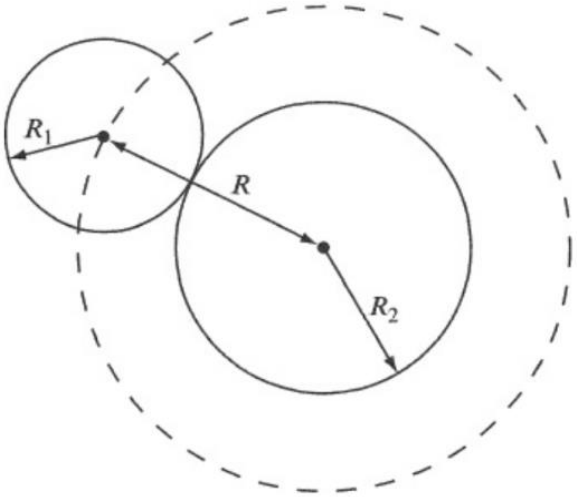

Figure 5 Representation of the effective nuclei as the sum of $R_1 + R_2$. The dotted line represents the cross-section region. Two nuclei approaching each other undergo nuclear collision if $R = R_1 + R_2$.

Both the effective radii and the interaction radius do not have definite value because of the range of the nuclear force but they are related to the geometric sizes of the nuclei. From experimental measurements we can estimate the value of R. The geometric cross-section for the uncharged particle is

$$\sigma = \pi R^2$$

The above cross section can be written in terms of wave number *K*, where $K = p / \hbar$. If L is the total angular momentum quantum number then

$$\begin{aligned} \sigma &= \pi (L / p)^2 \\ &= \pi l (l + 1) \hbar^2 / (\hbar K)^2 \\ &\sim \pi l^2 / K^2 \end{aligned}$$

In classical limit, $l >> 1$.

If the kinetic energy of the projectile is equal to the coulomb energy, then at lower energies the cross-section falls to zero because the nuclei are out of contact with each other. If the initial kinetic is less than the

coulomb energy, then even the particles are out of range classically but the cross-section remains finite. Because there is a possibility of the coulomb barrier penetration and therefore the nuclear reaction takes place. These are the classical or semiclassical approach for the estimation of the cross-section.

Quantum mechanical estimation

Classical estimation for cross-section is valid for the de Broglie wavelength comparable to the nuclear size or interaction radius R. We consider the quantum mechanical approach when the wavelength is comparable or greater than R.

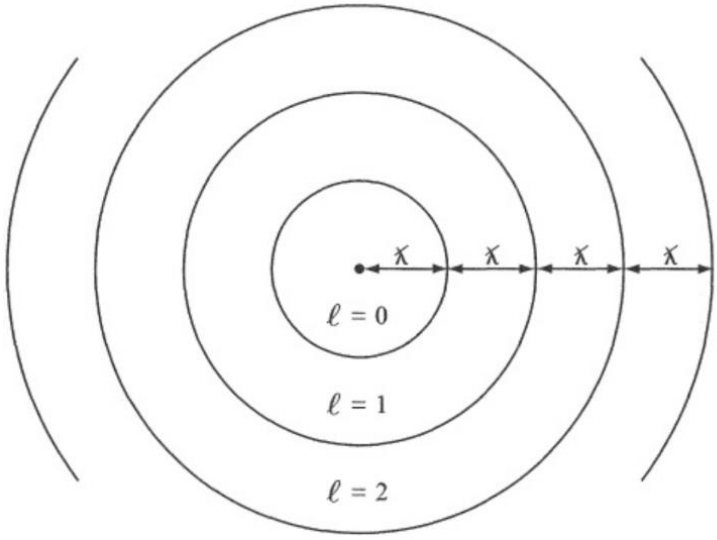

Figure 6 Division of interaction region of the approaching projectile into ring-shaped zone corresponding to the angular momentum *l*.

Quantum mechanically the cross-section is given by

$$\sigma_l = (2l + 1)\, \pi\, \lambda^2(\text{cut})$$

This cross-section is for the *l*th zone. Only integral values of *l* are allowed in quantum mechanics and angular momentum *l* corresponds to the *l*th zone. σ_l is the partial-wave cross-section. This equation represents the upper limit to the total cross-section. The reaction cross-section for the *l*th partial-wave is

$$\sigma_{r,l} \geq (2l + 1)\, \pi\, \lambda^2(\text{cut})$$

This equation is only applicable for the calculation of reaction cross-section. If the value of *l* is above zero, the overlapping of *l* zone with the nucleus decreases and effect of nuclear interaction on the partial-wave becomes negligible. If $l = 0$, we consider the slow neutron induced reactions where λ (cut) >> R. Some consequences of the reaction cross-section can be derived in the region where r > R.

In general, fusion cross-section is denoted by sigma(σ) and measured in barns.

Where,

$1\text{barn} = 10^{-24}\,\text{cm}^2 = 10^{-28}\text{m}^2$

When the two nuclei, whether they are deformed or spherical interact with each other the interaction takes place through coulomb and nuclear potentials. These potentials add up to give rise to a barrier which must be overcome for the fusion to initiate.

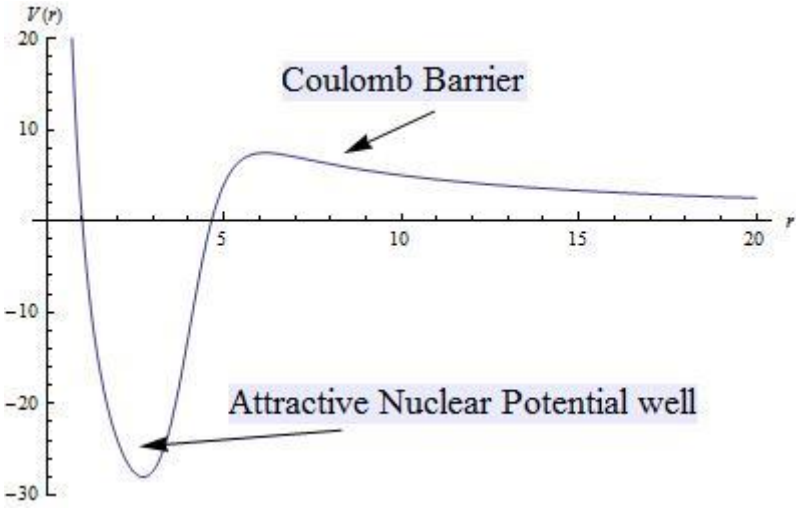

Figure 7 Short range attractive nuclear potential and coulomb barrier.

Conditions for the nuclear fusion to occur

- When the two nuclei interacting with each other have enough kinetic energy to overcome the coulomb barrier.

- If the interaction energy is smaller than the barrier energy, the nuclear fusion can take place through quantum tunnelling.

- The probability that fusion can take place depends upon the width of the barrier at that energy and this fusion decreases exponentially when the width of the barrier increases.

- At low energy the coulomb repulsion goes as 1/r that is coulomb barrier becomes very large that causes the difficulty in fusion to occur.

- To cause fusion the energy should be of the order of the MeV.

In order to calculate the fusion cross-section of light nuclei we take into account the nuclear potential. The nuclear potential taken is in the form of Woods-Saxon.

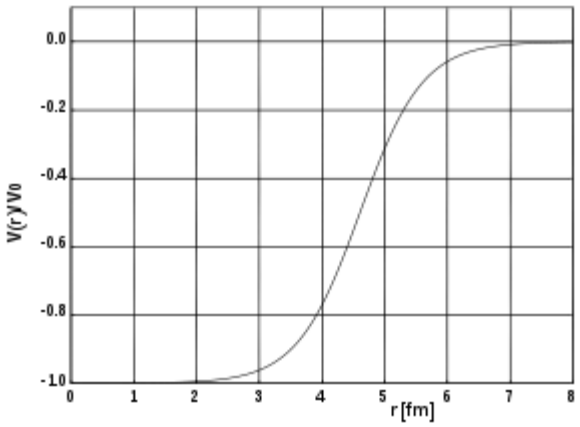

Figure 8 [ref 3]

The above figure 8 shows the Woods-Saxon potential for A=50, a = 0.5fm and R = 4.6fm

The Woods-Saxon approximately describes the force applied on nucleons for the structure of the nucleus. It is in the form of:

$$V(r) = \frac{Vo}{1+\exp(r-R)/a}$$

Where,

Vo = potential at center of the nucleus having dimensions of energy

a = constant(~0.5fm) representing the surface thickness of the nucleus

R = nuclear radius ($R = r_o A^{1/3}$)

It takes the form of potential well if atomic number A has higher values. Some characteristics are:

- With distance it increases monotonically.
- At higher values of A, it is approximately flat at the center.
- As nucleus is made up of nucleons, therefore nucleons that are present at the surface of the nucleus experience a great amount of force towards the center.
- As r goes to infinity it approaches to zero.

Comparison of Square-Well and Woods-Saxon Potential

- For Square-Well, r_o~1.35 fm to 1.6 fm.
- For Woods-Saxon with half potential radii, r_o~1.25 fm.
- For Woods-Saxon when there is decline from 90 to 10%, skin thickness of the full thickness when r_o~2.2 fm.

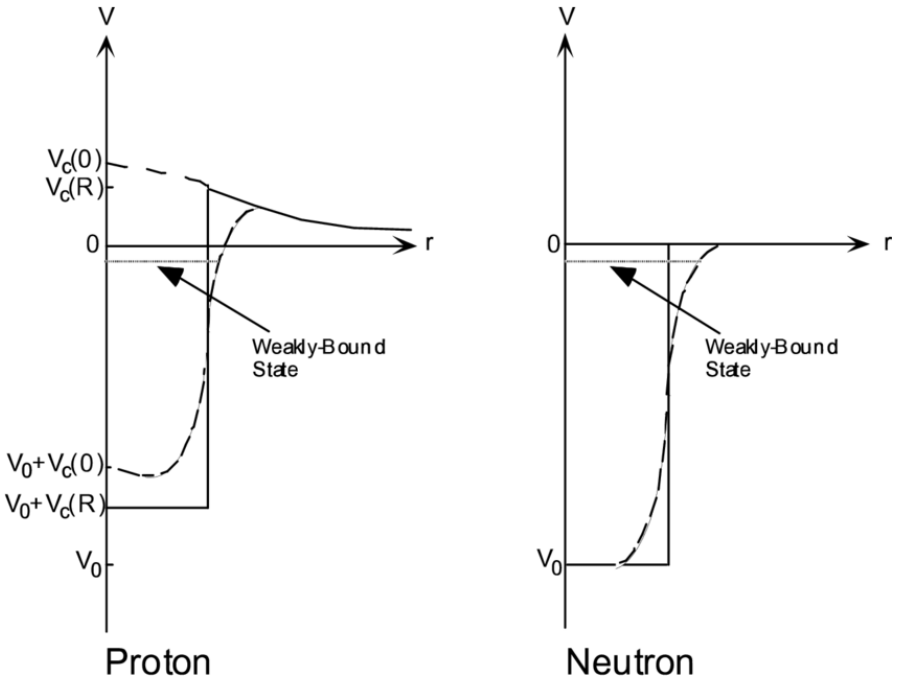

Figure 9 potential energy as a function of distance from the center of a nucleus for proton and neutron. The solid curve represents the square-well potentials and the dashed curves Woods-Saxon potentials. [Modern nuclear chemistry (Walter D. Loveland, David J. Morrissey, Glenn T. Seaborg)].

Chapter 2

2.1 Coupled channel calculations for heavy-ion fusion reactions

^{7}Li is a stable isotope of Li, which has a two-body cluster structure of α + t with breakup threshold at 2.47 MeV and bound excited at 0.478 MeV [4]. The breakup threshold is defined as the energy required to remove a nucleon from the nucleus. The breakup threshold is called as α-separation energy. If projectiles are weakly bound, then they give rise to many new reaction channels or opens many new processes like sequential complete fusion (SCF) In contrary, if projectiles are strongly bound then new reaction channels are not usually observed.
In order to measure the complete fusion (CF), we need to measure the sequential complete fusion and direct complete fusion. We can define complete fusion as the sum of two (CF = SCF + DCF) [5-10].
If a part of projectile is captured by the target nuclei, then it leads to incomplete fusion (ICF), which is in contrary to complete fusion. The sum incomplete fusion and complete fusion is called total fusion (TF).

In above-barrier region CF cross sections are supressed in comparison to TF, because of some loss of flux in ICF channels. While in below barrier region there is enhancement of both TF and CF [11-18].
We can perform, model calculations or run a program for coupled-channel calculations with all order couplings for heavy ion fusion reactions using CCFULL.
The program solves the coupled-channel equations to calculate the fusion cross-sections and mean angular momentum of compound nucleus by applying no-Coriolis approximation or iso-centrifugal approximation to reduce the dimensions of the channel coupling. No-

Coriolis approximation is a sudden tunnelling approximation related with the centrifugal energy and reduces the couple channel dimensions. Coupling interactions describes the inelastic excitations and transfer reactions. We perform coupled channels calculations in order to study the effect of inelastic excitations and transfer reactions on the fusion rate where the fusion process is governed by quantum tunnelling over the coulomb barrier.

Calculations has been performed using the modified version of CCFULL [19] which assumes that channel coupling to the ground state should be small and multi- nucleon transfer reactions should have much contribution in comparison to inelastic channels. We use Woods-Saxon parametrization of the Akyüz-Winther [20] potential with modified parameters to get rid of excitations at higher energies. In case of no-coupling it is used as 1DBPM excitation function. 1DBPM prediction reproduce the above-barrier measured value of TF but it underpredicts the below- barrier region values. When there is coupling to inelastic channels there is enhancement of fusion cross section in sub-barrier energies, but this model underpredicts the CF data in the below -barrier region.

2.2 ***Coupled-channel equations***

Below-barrier energies and above-barrier energies involve the strongest coupling effects and so many energies are involved at energies high above the barrier [21]. Ignoring the transfer reaction, for simplicity we consider the coupling to inelastic channels. For the interaction between the nuclei, the Hamiltonian is described as

$$H = -\frac{\hbar^2}{2\mu} \bigtriangledown^2 + h(\xi) + V_0(r) + V_{coup}(r, \xi) \qquad (1)$$

In this above equation h(ξ) is the internal Hamiltonian for the target nucleus and ξ stands for internal dynamical variable. V_{coup}(r, ξ) is the coupling term which describes the coupling between the relative motion and internal degree of freedom. V_0(r) is the bare potential which depends upon distance r. Then the wave function which depends upon r and ξ has the form

$$\left(-\frac{\hbar^2}{2\mu}\nabla^2 + h(\xi) + V_0(r) + V_{coup}(r,\xi)\right)\Psi(r,\xi) = E\Psi(r,\xi)$$

(2)

Now in each channel we replace the angular momentum of the relative motion by the total angular momentum [1,2], then we read coupled-channel equations as

$$\left[-\frac{\hbar^2}{2\mu}\frac{d^2}{dr^2} + \frac{J(J+1)\hbar^2}{2\mu r^2} + V_N^{(0)}(r) + \frac{Z_P Z_T e^2}{r} + \epsilon_n - E\right]\psi_n(r) + \sum_m V_{nm}(r)\psi_m(r) = 0,$$

(3)

Here μ is the reduced mass, *r* is the radial component of the relative motion. ϵ_n is the excitation energy of the nth channel and E and V_{mn} is called as the bombarding energy in the center of mass frame and the matrix elements of the coupling Hamiltonian. $V_N^{(0)}$ is the nuclear potential in the incoming wave channel.

The Woods-Saxon parametrisation for nuclear potential $V_N^{(0)}$ is

$$V_N^{(0)}(r) = -\frac{V_0}{1+\exp((r-R_0)/a)}, \qquad R_0 = r_0(A_P^{1/3} + A_T^{1/3}),$$

(4)

By applying the boundary conditions, we can solve the coupled-channel equations in which the incident channel is composed of incoming wave at $r = r_{min}$ and outgoing wave at infinity except the entrance channel that is at n = 0, while all other channels consist of

only outgoing wave. As the imaginary potentials suppress the coupling therefore it is not suited to study the channel coupling effects on barrier penetration but by imposing the incoming wave boundary condition (IWBC) [22] we can remove the strongly absorbing potential in the coupled equations. The boundary conditions are

$$\begin{aligned} \psi_n(r) &\rightarrow T_n \exp\left(-i\int_{r_{\min}}^{r} k_n(r')dr'\right) && r \le r_{min}, \\ &\rightarrow H_J^{(-)}(k_n r)\delta_{n,0} + R_n H_J^{(+)}(k_n r) && r > r_{\max}, \end{aligned} \tag{5}$$

Here k_n is the local wave number for the nth channel which is expressed as

$$k_n(r) = \sqrt{\frac{2\mu}{\hbar^2}\left(E - \epsilon_n - \frac{J(J+1)\hbar^2}{2\mu r^2} - V_N(r) - \frac{Z_P Z_T e^2}{r} - V_{nn}(r)\right)} \tag{6}$$

When r equals to infinity

$k_n = k_n(r = \infty)$

$H_J^{(-)}$ and $H_J^{(+)}$ in the above equation are coulomb functions of the incoming wave and outgoing wave. As there are only incoming wave at $r = r_{\min}$, therefore the program solves the channel equations outwards from $r_{\min}$ by setting [23]

$$\begin{aligned} &\psi_n(r_{\min}) = 1, \qquad \psi_m(r_{\min}) = 0 \quad (m \neq n), \\ &\frac{d}{dr}\psi_n(r_{\min}) = -ik_n(r_{\min}), \qquad \frac{d}{dr}\psi_m(r_{\min}) = 0 \quad (m \neq n). \end{aligned} \tag{7}$$

In the above equation the first derivative of the wave function has been determined from Eq. (3) at $r = r_{\min}$. The wave function at $r = r_{\min} + h$ can be calculated by RK method. When we determine the wave function at $r = r_{\min} + h$, CCFUL then solves the coupled-channel equations from $r = r_{\min} + h$ to $r = r_{\max}$ by modified Numerov methods

[24] as CCFUL directly solves the second order coupled-channel equations ny modified Numerov method. The modified Numerov method connects the wave functions at $r_{i+1} \equiv r_{min} + (i+1)\,h$ to r_i and r_{i-1} as

$$\psi^{i+1} = \left(1 - \frac{h^2}{12}\mathcal{A}^{i+1}\right)^{-1}\left[\left\{\left(\frac{h^2}{\sqrt{12}}\mathcal{A}^i + \sqrt{3}\right)^2 - 1\right\}\left(1 - \frac{h^2}{12}\mathcal{A}^i\right)\psi^i - \left(1 - \frac{h^2}{12}\mathcal{A}^{i-1}\right)\psi^{i-1}\right], \tag{8}$$

Now the equation given below satisfies the boundary condition (5) at $r = r_{min}$.

$$\psi_m(r) = \sum_n T_n \chi_{nm}(r). \tag{9}$$

Let $\chi_{nm}(r)$ be the wave function of the m^{th} channel. Now at $r = r_{max}$

$$\chi_{nm}(r) = C_{nm} H_J^{(-)}(k_m r) + D_{nm} H_J^{(+)}(k_m r) \qquad r \to r_{max}. \tag{10}$$

Eq. 9 at $r = r_{max}$ becomes

$$\psi_m(r_{max}) = \sum_n T_n \chi_{nm}(r_{max}) = \sum_n T_n \left(C_{nm} H_J^{(-)}(k_m r_{max}) + D_{nm} H_J^{(+)}(k_m r_{max})\right). \tag{11}$$

On comparing equation at $r > r_{max}$ and eq. 11, we get

$$\sum_n T_n C_{nm} = \delta_{m,0}. \tag{12}$$

Where T_n is called the transmission coefficient which is obtained by

$$T_n = \left(C^{-1}\right)_{n0}. \tag{13}$$

Our interest is only in inclusive process in which the intrinsic degree of freedom emerges in any final state. Then when we sum over all the intrinsic states, gives the inclusive penetrability as

$$P_J(E) = \sum_n \frac{k_n(r_{\min})}{k_0} |T_n|^2 .$$

(14)

Then at last fusion cross section and mean angular momentum of the compound nucleus are calculated by the equations given below

$$\sigma_{fus}(E) = \sum_J \sigma_J(E) = \frac{\pi}{k_0^2} \sum_J (2J+1) P_J(E),$$

(15)

$$\begin{aligned} < l > &= \sum_J J\sigma_J(E) / \sum_J \sigma_J(E), \\ &= \left(\frac{\pi}{k_0^2} \sum_J J(2J+1) P_J(E) \right) \Big/ \left(\frac{\pi}{k_0^2} \sum_J (2J+1) P_J(E) \right) \end{aligned}$$

(16)

From equation 16, we conclude that the summation over the partial wave is truncated at the angular momentum whose contribution to the cross-section is less than 10^{-4} the total cross-section.

2.3 Matrix elements of coupled channel

The program CCFUL treats a vibrational coupling in the harmonic limit and a rotational coupling with a pure rotor.

Rotational coupling

Consider the rotational coupling in the target nucleus, then by changing the target nucleus in the nuclear potential (2) to a dynamical operator

$$R_0 \rightarrow R_0 + \hat{O} = R_0 + \beta_2 R_t Y_{20} + \beta_4 R_t Y_{40}, \tag{17}$$

Here β_2 and β_4 are the quadrupole and hexadecapole deformations and radius of the target nucleus is parametrised as $r_{coup}\ A_T^{1/3}$ respectively. Then the nuclear coupling Hamiltonian is

$$V_N(r, \hat{O}) = -\frac{V_0}{1 + \exp((r - R_0 - \hat{O})/a)}. \tag{18}$$

Vibrational coupling

The all order nuclear couplings for the case where the vibration can be approximated by the harmonic oscillator is discuss in reference [26]. In some realistic cases the phonon spectra truncated at some level which results in the deviation of the intrinsic motion from the harmonic limit even at equally spaced excitation energies [27]. The nuclear Hamiltonian operator for the vibrational coupling is given by

$$\hat{O} = \frac{\beta_\lambda}{\sqrt{4\pi}} R_t (a^\dagger_{\lambda 0} + a_{\lambda 0}), \tag{20}$$

In the above equation λ is the multipolarity of the vibrational mode and $a_{\lambda 0}^\dagger(a_{\lambda 0})$ is the annihilation operator of the phonon.

Transfer coupling

This program includes the transfer-pair coupling between the ground states and make use of macroscopic factor with coupling strength F_T which is given by [28]

$$F_{trans}(r) = F_t \frac{dV_N^{(0)}}{dr}, \tag{23}$$

However, fusion cross-section shows anomalous behaviour in close vicinity of the coulomb barrier. It is observed that the fusion cross-section shows much larger value than expected from the 1DPM [29-35]. This enhancement in the value of fusion cross-section is may be due to some physical changes taking place in the tunnelling region. Static deformation coupling to the low-lying excited states and neutron transfer reactions are responsible for the enhancement of the magnitude of the sub-barrier fusion cross-section, therefore, enhancement is more pronounced for the deformed nuclei in the sub-barrier regions. In quadrupole deformation the barrier height is lowered in the elongation direction. An enhancement factor is observed when axis of deformation is parallel to the collision axis and the reduction factor is observed when the axis of deformation is perpendicular to the collision axis. The height of the barrier depends upon the angle of orientation of the deformed nuclei.

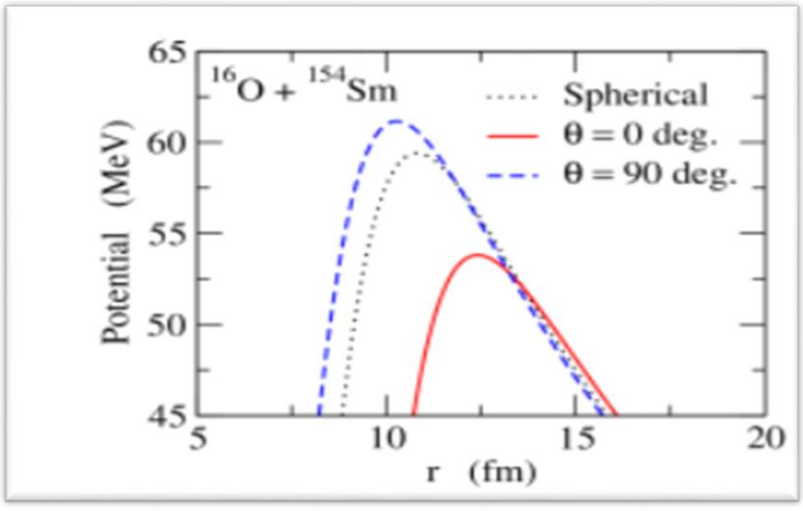

Figure 10 The figure shows the different barriers associated with different angles of orientation of deformed nuclei. [ref 33]

Vibrational and rotational excitations modify the tunnelling probability and dependence of sub-barrier fusion excitation functions.

When there is deformation in the spherical nuclei due to low lying surface vibrations, the barrier height decreases and sub-barrier fusion cross-section increase. For simplicity we use Woods-Saxon potential with radius, depth and diffuseness as parameters. Now, we will analyse how these parameters affect our fusion cross-section by changing their values.

Chapter 3

3.1 *Effect of nuclear potential parameters on fusion cross section*

Fusion cross section depends upon nuclear potential around the barrier. The width of the fusion barrier and the coupling strengths are affected by the nuclear potential. We use modified Woods-Saxon form, which is defined by three main parameters: the potential depth, the diffuseness and the radius. Any change in the values of these three parameters changes the fusion cross section. In this we change the value one parameter by keeping the two parameters value constant.

3.1.1 Effect of change in diffuseness parameter on fusion cross section

Any change in the diffuseness parameter affects the coupling strength and the width of the barrier [36]. It is denoted by 'a' or 'a_0'. The commonly accepted value of 'a' of the Woods-Saxon is equivalent to 0.65 fm. The higher values or lower values of diffuseness parameter from the commonly accepted value directly affects the width of the barrier and coupling strengths. The fusion barrier is no longer defined when we make use of very large values of angular momenta because in such case the potential pocket becomes shallower and the fusion barrier disappears and fusion does not take place. But in CCFULL we apply the incoming wave boundary condition at $r = r_{min}$, and that's why we need deeper potentials for large values of 'a'. We can also include the other parameter along with the above three parameters which is

energy dependent parameter. But we will take this parameter into account through diffuseness parameter.

Dependence of diffuseness parameter

Diffuseness parameter depends upon *l*-values or angular momentum values. Larger *l*-value means that the barrier height therefore in such case fusion process do not contribute.

Secondly, there may be modification in the value of diffuseness parameter due to effect of friction at higher angular momenta. As there is conflict between the fusion and dissipative reactions which leads to reduction in the fusion cross-section and therefore in order to fit the fusion cross-section large value of the diffuseness parameter is required [37].

The total potential is the sum of the nuclear potential and the coulomb potential energies. Fusion takes place when the projectile overcomes the fusion barrier and enters the potential well.

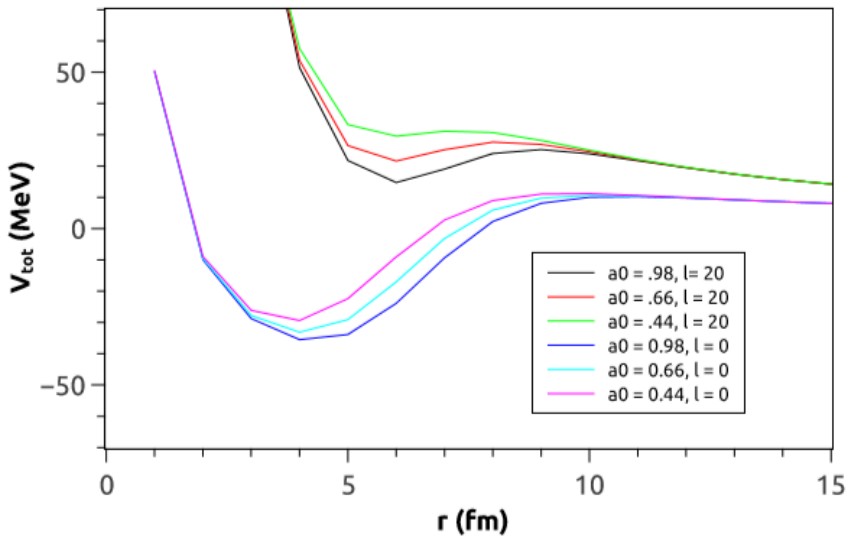

Figure 11. The internuclear potential V_{tot} as a function of r of the reaction ^{7}Li with ^{64}Ni for angular momentum values of 0 and 20 keeping V_0 and r_0 fixed at 71.4 MeV and 1.1 fm respectively.

Figure 11 shows that for large values of angular momentum the potential pocket becomes shallow and disappears at $l \geq 60$. Calculations are sensitive to ion-ion potential in the interior. When we compare a_0 at l = 0 and l = 20, potential pocket is deep for large values of diffuseness parameter and becomes shallower for small diffuseness parameter.

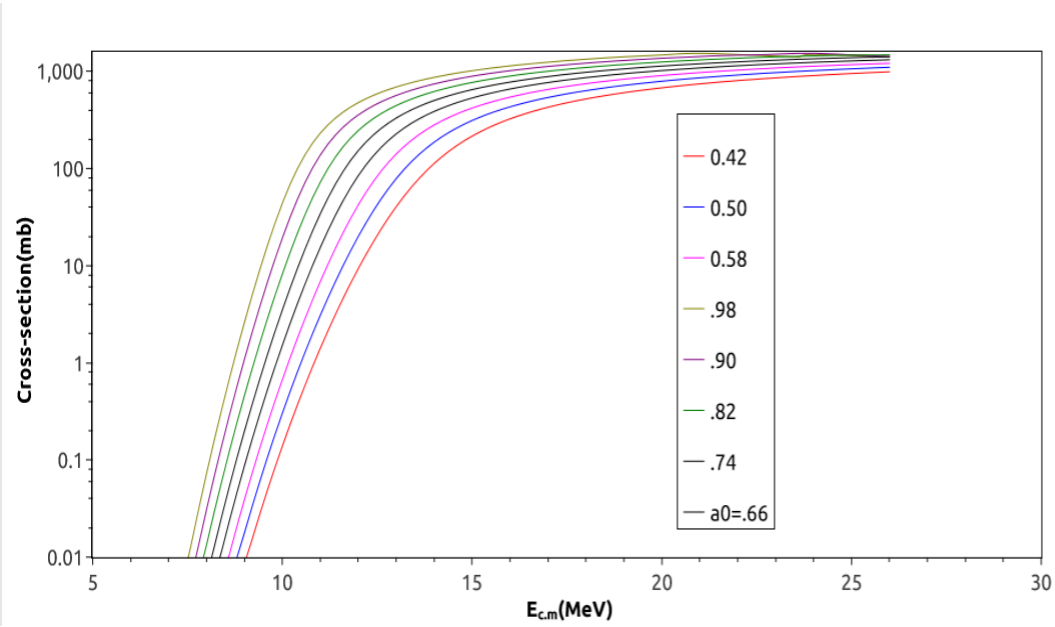

Figure 12. Variation of fusion cross-section with diffuseness parameters

The above graph shows the change in the fusion cross-section by changing the value of diffuseness parameter in case of spherical nuclei. Here we have taken the standard value of diffuseness parameter as 0.66 by keeping the potential fixed at 71.2 and radius at 1.02. From this standard value we increase the parameter by 0.08 units up to 0.98 and decrease the parameter by 0.08 units up to 0.38. Therefore, the variation in the diffuseness parameter is from 0.38 to 0.98 by taking the standard value as 0.66. The graph shows that when we take the value of diffuseness parameter as 0.38, the fusion cross-

section is lowest and when we increase the value from 0.42, the cross-section starts increasing and is maximum at 0.98. Therefore, by increasing the value of diffuseness parameter the fusion cross-section also increases and by decreasing the value of diffuseness parameter from the standard value the fusion cross-section decreases. The reason behind this is that barrier curvature is inversely proportional to the square of the diffuseness parameter [38-43]. Hence, by decreasing the value of diffuseness parameter the barrier curvature increases which decreases the fusion process and hence fusion cross-section decreases. Similarly, if we increase the value of diffuseness parameter the barrier curvature decreases which increases the fusion process and hence fusion cross-section increases.

So, any change in the diffuseness parameter leads to the variation in the tunnelling region between the colliding nuclei.

In case of deformed nuclei

The deformation arises because of the way valence nucleons arrange themselves in an unfilled subshell and the deviation from sphericity is about 20%.

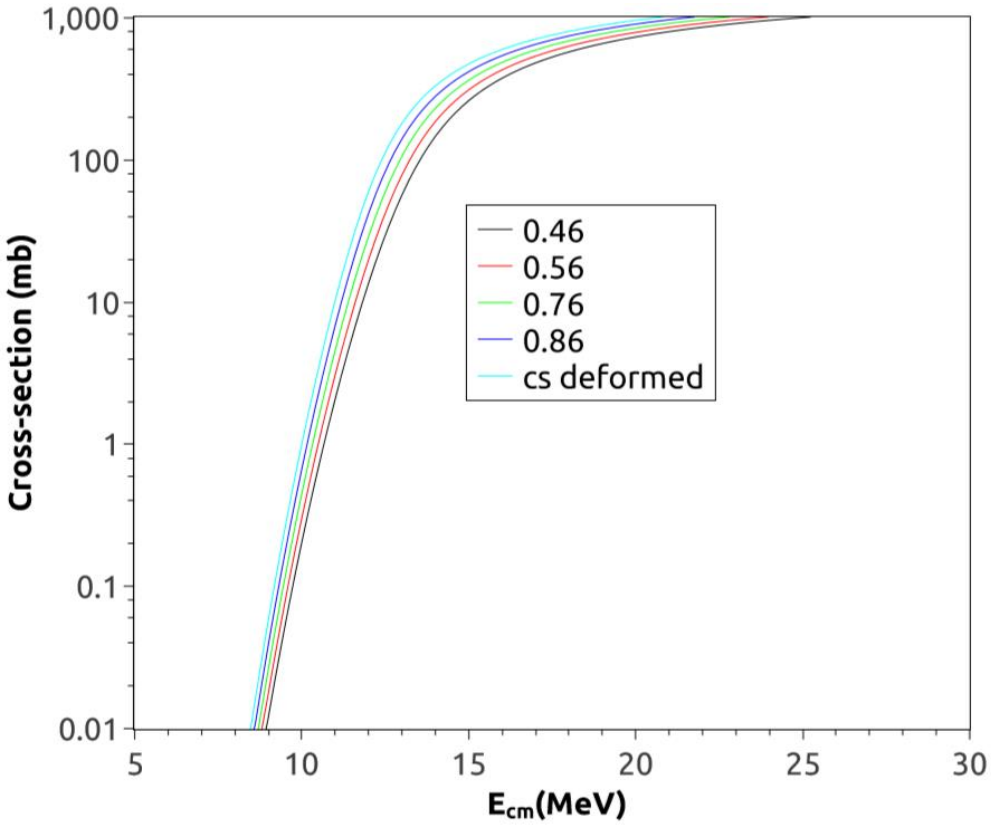

Figure 13 Variation in the fusion cross-section in case of deformed nuclei.

In this case the nucleus is deformed due to vibrational coupling of the target. The figure 13 shows that if the target is deformed, the fusion cross-section increases. The quadrupole deformation (β_2) and octupole deformation (β_3) and their orientation with the colliding axis affect the fusion barriers and hence the fusion cross-section. Orientation of the deformed nuclei effect the barrier height, barrier position, the depth and shape of nuclear potential well. In case of light nuclei, the effect of quadratic term in the quadrupole deformation and averaging over the angle are small as the averaging over the angle also affects the sub barrier energies and the barrier height. The result of the deformation is that the fusion cross-section barrier near the barrier energy of spherical, deformed and nearly spherical is strongly enhanced. The enhancement factor is denoted by EF and is defined as

$$(EF)_i = \frac{\sigma_i}{\sigma_{1DBPM}}, \qquad i = TF, CF, CC, 1DBPM, \ldots$$

The experimentally calculated enhancement factor for total fusion TF, complete fusion CF and coupled channel CC is shown in figure 13 below

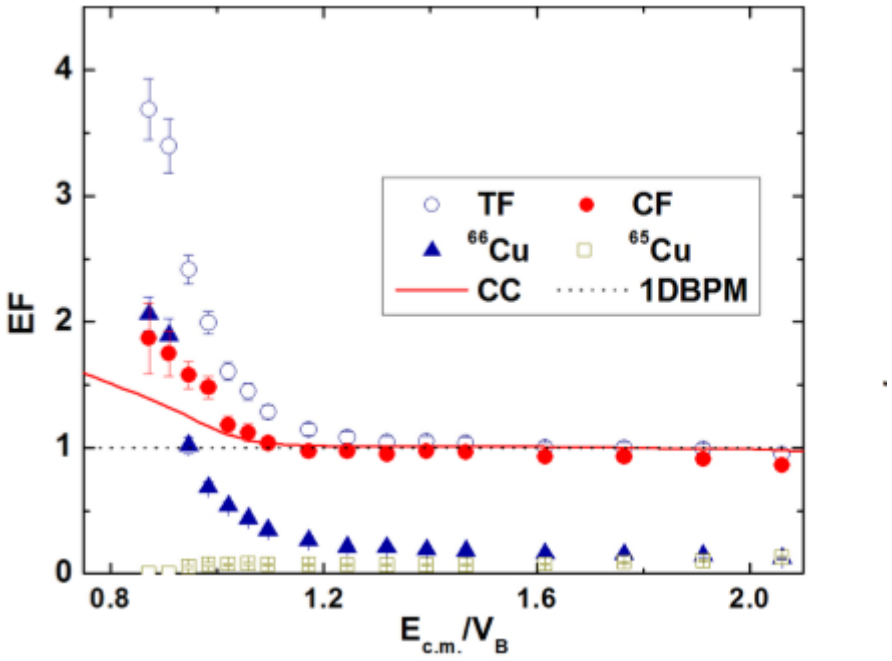

Figure 14 The enhancement factor for TF, CF and CC cross sections relative to 1DBPM cross-sections plotted as a function of E_{cm}/V_B, V_B at 1.18 (physical review C **93**, 044616)

This graph shows that the enhancement factor for CF is suppressed as compared to TF and CC enhancement factor. Also, the TF enhancement is steeper at region below 1 in comparison to CF cross-section enhancement. But the suppression of $(EF)_{CF}$ in the above barrier region is not so prominent as compared to the enhancement in the below barrier energies. The ^{66}Cu and ^{65}Cu are the residues of the reaction. The very small cross-section of ^{65}Cu shows that at sub barrier energies the one proton stripping does not play significant role and have no contribution.

In order to explain the fusion cross-section at energies above the barrier, the required diffuseness is approx. 1.5 times the commonly accepted value and at energies below the barrier the fusion cross-section is found to fall steeply. But when we take the large value of diffuseness parameter it again become uniform or unvarying.

These observation shows that when we take the large values of diffuseness parameter it can explain both the above barrier and below barrier fusion data.

3.1.2 Effect of change in potential parameter on fusion cross-section

The Woods-Saxon nuclear potential V_{nuc} is defined as

$$V_N^{(0)}(r) = -\frac{V_0}{1+\exp((r-R_0)/a)}, \qquad R_0 = r_0(A_P^{1/3} + A_T^{1/3}),$$

Here V_0 is the depth of the potential, r_0 is the radius and *a* is the diffuseness parameter. *r* is the center-of-mass distance between the projectile and the target mass number A_P and A_T. In this case we will change the potential parameter by keeping the two other parameters: the diffuseness and the radius fixed and observe how the potential parameter affect the fusion cross-section.

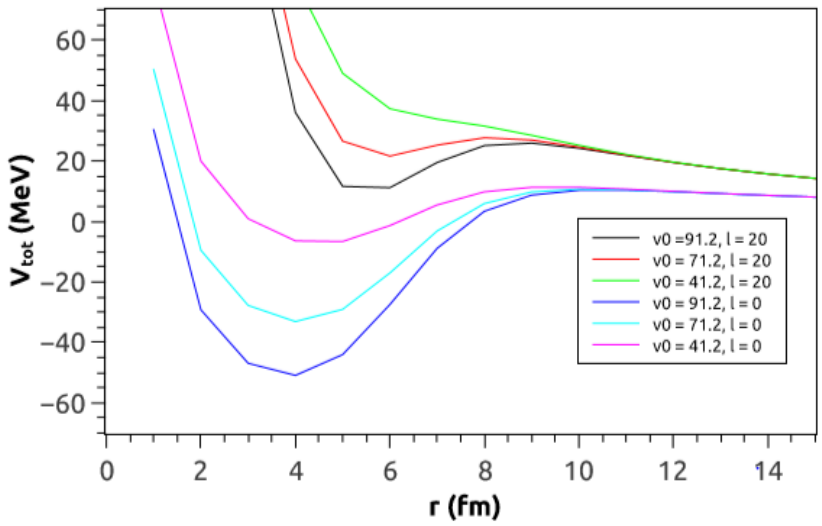

Figure 15. The internuclear potential V_{tot} as a function of r for the reaction ^{7}Li with ^{64}Ni for angular momentum values of 0 and 20 keeping a_0 and r_0 fixed at 0.66 fm and 1.1fm respectively.

The graph in the figure 15 shows that as potential depends upon the fusion barrier radii, the potential pocket becomes shallower for small values of potential parameter and for large values of angular momentum. When we compare V_o at l = 0 and l = 20 and the fusion barrier radii are smaller for small angular momentum. Coulomb term becomes significant in case of shallow potential pocket.

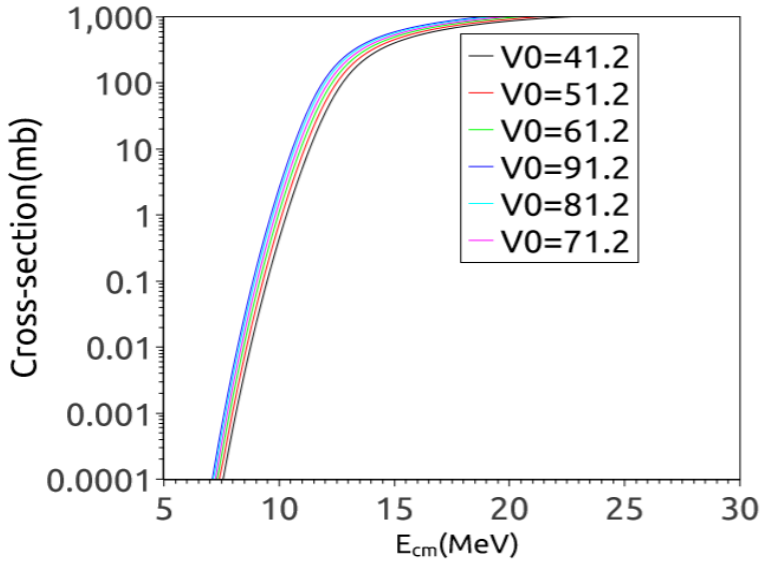

Figure 16. Variation in cross-section with variation in potential parameter.

The above figure 16 shows that when we change the potential from the standard value, the fusion cross-section also vary. Here we have taken the standard potential as 71.2 for calculation of fusion cross of ^{7}Li with ^{60}Ni. This depth has been choosen such that total potentential is greater than Q-value of the fusion reaction. The radius *r* is fixed at 1.02. The observation from the graph shows that when we increase the depth of the potential (V_0) from the standard value, the fusion cross-section enhance and if we decrease the potential depth from the standard value, there is decrement in the fusion cross-section barrier. The reason behind this is that:

All these observation shows that when we take the deeper potential by keeping the diffuseness parameter and the radius parameter fixed, the fusion cross-section increases and energy at deeper potential decreases. But using the deeper potential hides the physical effects which causes fusion to occur even when there is absence of attractive potential pocket.

3.1.3 Effect of change in radius parameter on fusion cross-section

The last parameter on which the Woods-Saxon potential depend is on the radius of the nuclear potential. The change in radius also affects the fusion-cross section. In this we change the radius parameter by keeping the other two parameters: the diffuseness and potential fixed at there standard values (a = 0.70 and V_0 = 71.2).

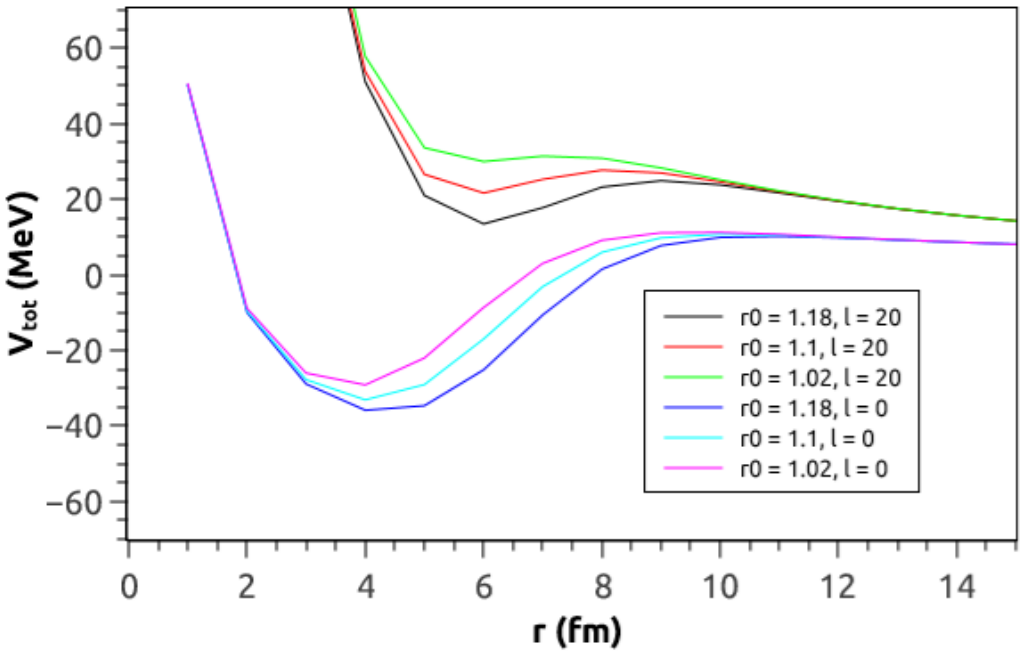

Figure 17. The internuclear potential V_{tot} as a function of r for the reaction of ^{7}Li with ^{64}Ni for angular momentum values of 0 and 20, keeping V_0 and a_0 fixed at 71.4 MeV and 0.66 fm respectively.

The results in the above graph shows that when we increase the value of fusion radii r, the potential pocket becomes deeper. When we compare r_0 at l = 0 and l = 20, the potential pocket becomes more shallower at higher values of angular momentum which decreases the fusion cross-section rate.

The graph 18 below shows the effect on fusion cross-section by changing the radius parameter.

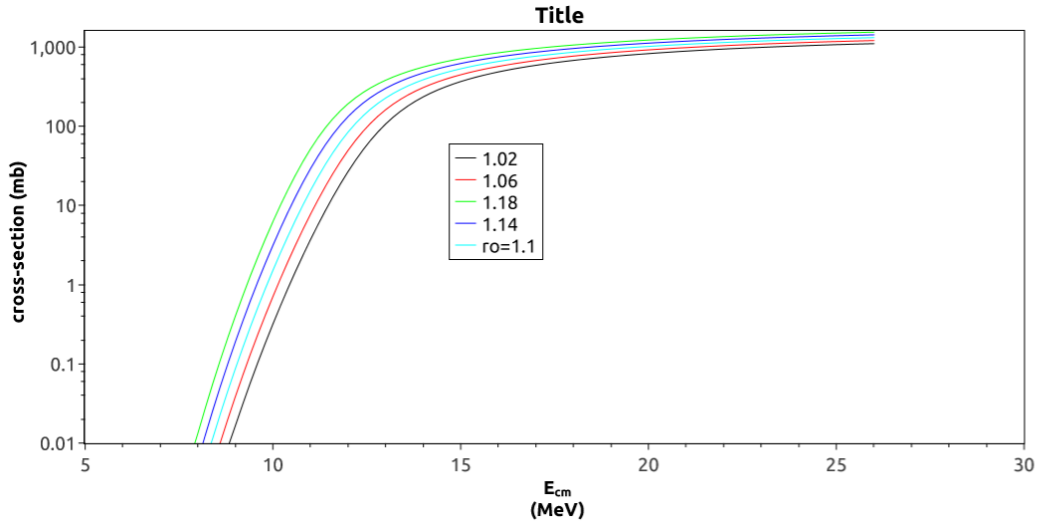

Figure 18. Variation in the fusion cross-section by varying radius parameter.

The observation shows that when we increase the value of radius parameter from the standard value, the fusion cross-section increases and vice-versa. This is due to the reason that when we increase the radius of the potential, the potential pocket becomes deeper (shown in figure 17) which increases the fusion rate, therefore fusion cross-section increases.

Hence at smaller radii the potential pocket become shallower and the coulomb term becomes significant.

3.2 ***Comparison of the fusion cross-section for the deformed and the spherical nuclei***

In order to study nuclear reactions experimentally deformed nuclei are frequently used. The reactions between deformed nuclei is our topic of interest. The graph 16 given below shows the fusion cross-section for the deformed and the spherical nuclei.

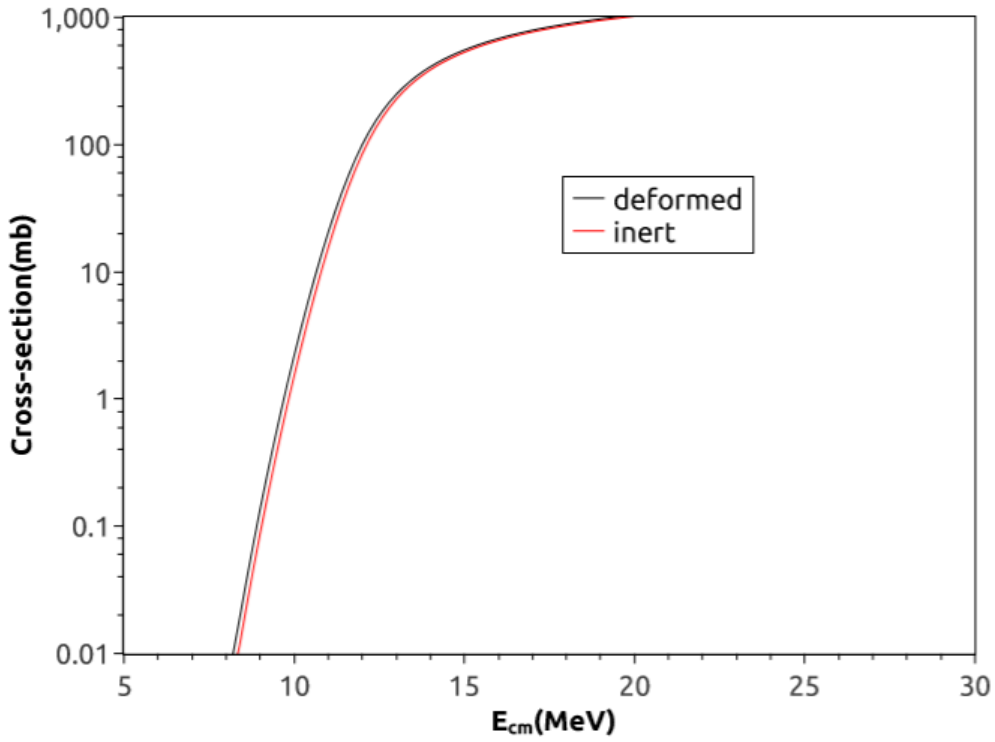

Figure 19. Variation in fusion cross-section in case of deformed and inert nuclei.

The observation shows that the fusion cross-section for the deformed nuclei is greater than the fusion cross-section for the spherical nuclei. The inclusion of the coupling by considering the vibrational deformations enhances the calculation around and below the coulomb barrier.

In case of weakly bound system, the fusion barrier data for the weakly bound projectiles like ^{6,7}Li and stable isotope of beryllium show enhancement in the fusion cross-section but this enhancement is not so strong. At above barrier energies, when these projectiles collide with the heavy targets the experimental cross-section is suppressed by 30%. And in case of collision with the medium mass targets this suppression is smaller and there is no effect in collision with the light mass targets.

When we study the sub barrier fusion reactions, the value of cross-section exceeds the prediction of the model of one-dimensional

tunnelling. In order to explain the enhancement of the fusion cross-section at sub barrier energies various models and mechanisms were proposed.

The orientation of the deformed nuclei also affects the barrier height, shape of the potential well and hence the fusion cross-section. As the fusion cross-section depends on the barrier height, therefore orientation effects play a major role in calculating the cross-section for the deformed nuclei. Hence, we conclude that:

- The fusion cross-section for spherical nuclei is smaller than the deformed nuclei because there is no coupling effect in case of spherical nuclei. And in case of deformed nuclei the coupling reduces the barrier height and increases the fusion cross-section.
- Any variation in the orientation of the deformed nuclei changes the barrier height, its position, the depth and shape of the potential well.
- In case of lighter nuclei, the quadratic term in quadrupole deformation and averaging over the angle effects are small. But as we increase the charge and the mass of the nuclei, averaging over the angle effects the fusion cross-section at sub barrier energies and also effects the barrier height.
- If the deformation is prolate, it strongly effects both the nuclear potential and the fusion cross-section for heavy and lighter nuclei. But if the deformation is oblate, it effects both the nucleus-nucleus potential and the fusion cross-section in case of heavy nuclei systems.

Chapter 4

Literature review [Physical Review C **82**, 014614 (2010)]

- *Research purpose*

  The main purpose of his work is to determine the fusion excitation function above and below the coulomb barrier. He measured the cross-section from 1μb up to 500 mb. The data was available on ^{58}Ni + ^{60}Ni which indicated the influence of vibrational coupling on ^{58}Ni + ^{54}Fe. He made use of Couple channel calculations (CC) using Woods-Saxon potential in the measured energy range and including quadrupole and octupole phonons which give the information about ^{58}Ni + ^{54}Fe. As there was no good knowledge of multi phonon states specially in case of heavy and medium mass systems where the multi phonon states play a major role in enhancement of the fusion cross-section, he used different potentials. One of them was the ion-ion potential which was similar to AW potential having potential depth V_0 at 81.2 MeV, diffuseness parameter (*a*) equals to 0.67 fm and radius parameter (r_0) equals to 1.15 fm. The second potential was with the large diffuseness parameter *a* = 0.90 fm and potential depth and radius at 107.2 MeV and 1.05 fm respectively. By taking these two different potentials he observed that whether V_0 is 81.2 MeV or V_0 is 107.2 MeV, both the potentials produce potential barrier (V_b) at 94.0 MeV which was 1.3 MeV higher than barrier produced by AW and enables the good fit of the fusion cross-section at higher energies.

  The CC calculations performed by him give the detailed information about the excitation function above and below the barrier [53]. The potential similar to AW was used for the calculation of excitation function of ^{58}Ni + ^{54}Fe. For a good fit of cross-section above the barrier energies, he slightly varied the radius and potential. In second

potential (CC), he used the large diffuseness parameter and kept on varying the radius and depth of the potential parameter in order to obtain the same barrier height and kept the diffuseness parameter at 0.67 fm which produced a thicker barrier that lead to decrease of the excitation function at low energies and hence stimulates the fusion hinderance. But there was no slope in the region below the barrier either with *a* at 0.67 fm or *a* at 0.90 fm showing the steeper decrease of the fusion cross-section for large diffuseness below 87 MeV energy.

Conclusion of his work

The standard Woods-Saxon potential was used for coupled channel calculations which gave us the information of the excitation function for the cross-section of about 180μb. The fusion cross-section decreased at lower energies because at lower energies fusion hindrance plays a major role. This fusion cross-section can be reproduced by taking into account the large diffuseness parameter with WS shape of the ion-ion potential. CC calculations start over estimating the fusion cross-section at threshold energies because at threshold energy the barrier distribution vanishes.

References

[1] K. Hagino, N. Takigava, A.B. Balantekin, J.R. Bennett, Phys. Rev. C 52 (1995) 286.

[2] R. Lindsay, N. Rowley, J. phys. G 10 (1984) 805.

[3] Flugge, Sieg fried (1999). Practical Quantum Mechanics. Springer Berlin Heidelberg. pp. 162 ff.

[4] M. Dasgupta, D.J. Hinde, J.O. Newton and K. Hagino, The nuclear potential in heavy ion

[5] M. Dasgupta, D.J. Hinde, K. Hagino, S.B. Moraes, P. R. S. Gomes, R. M. Anjos, R.D. Butt, A.C. Berriman, N. Carlin, C. R. Morton, J. O. Newton, and A. Szanto de Toledo, Phys. Rev. C 66, 041602(R) (2002)

[6] M. Dasgupta, P. R. S. Gomes, D. J. Hinde, S. B. Moraes, R. M. Anjos, A. C. Berriman, R. D. Butt, N. Carlin, J. Lubian, C. R. Morton, J. O. Newton, and A. Szanto de Toledo, Phys. Rev. C 70, 024606 (2004).

[7] C. S. Palashetkar, Shital Thakur, V. Nanal, A. Shrivastava, N. Dokania, V. Singh, V.V.Parker, P.C. Rout, R. Palit, R. G. Pillay, S.Bhattacharyya, A. Chatterjee, S. Santra, K. Ramachandran, and N. L. Singh, Phys. Rev. C 89, 024607 (2014).

[8] Vandana Tripathi, A. Navin, K. Mhata, K. Ramachandran, A. Chatterjee, and S. Kailas, Phys. Rev. Lett. 88, 172701 (2002).

[9] A. Mukherjee, Subinit Roy, M. K. Pradhan, M. Saha Sarkar, P. Basu, B. Dasmahapatra, T. Bhattacharya, S. Bhattacharya, S. K. Basu, A. Chatterjee, V. Tripathi, and S. Kailas, Phys. Lett. B 636, 91 (2006).

[10] P. K. Rath, S. Santra, N. L. Singh, B. K. Nayak, K. Mahata, R. Palit, K. Ramachandran, S. K. Pandit, A. Parihari, A. Pal, S. Appannababu, Sushil K. Sharma, D. Patel, and S. Kailas, Phys. Rev. C 88, 044617 (2013).

[11] D. J. Hinde, M. Dasgupta, B. R. Fulton, C. R. Morton, R. J. Wooliscroft, A. C. Berriman, and K. Hagino, Phys. Rev. Lett. 89, 272701 (2002).

[12] P. R. S. Gomes, I. Marti, M. D. Rodr´ıguez, G. V. Mart´ı, R. M. Anjos, J. Lubian, R. Veiga, R. Liguori Neto, E. Crema, N. Added, L. C. Chamon, J. O. Fern´andez Niello, O. A. Capurro, A. J. Pacheco, J. E. Testoni, D. Abriola, A. Arazi, M. Ram´ırez, and M. S. Hussein,Phys. Lett. B 601, 20 (2004).

[13] A. Di Pietro, P. Figuera, E. Strano, M. Fisichella, O. Goryunov, M. Lattuada, C. Maiolino, C. Marchetta, M. Milin, A. Musumarra, V. Ostashko, M. G. Pellegriti, V. Privitera, G. Randisi, L. Romano, D. Santonocito, V. Scuderi, D. Torresi, and M. Zadro, Phys. Rev. C 87, 064614 (2013).

[14] Md. Moin Shaikh, Subinit Roy, S. Rajbanshi, M. K. Pradhan, A. Mukherjee, P. Basu, S. Pal, V. Nanal, R. G. Pillay, and A. Shrivastava, Phys. Rev. C90, 024615 (2014).

[15] C. Beck et al., Phys. Rev. C 67, 054602 (2003).

[16] Mandira Sinha, H. Majumdar, P. Basu, Subinit Roy, R. Bhattacharya, M.Biswas, M.K.Pradhan, R.Palit, I.Mazumdar, and S. Kailas, Eur. Phys. J. A44, 403 (2010).

[17] M. Ray, A. Mukherjee, M. K. Pradhan, Ritesh Kshetri, M. Saha Sarkar, R. Palit, I. Majumdar, P. K. Joshi, H. C. Jain, and B. Dasmahapatra, Phys. Rev. C 78, 064617 (2008).

[18] A. Mukherjee, U. Datta Pramanik, S. Chattopadhyay, M. Saha Sarkar, A. Goswami, P. Basu, S. Bhattacharya, M. L. Chatterjee, and B. Dasmahapatra, Nucl. Phys. A 645, 13 (1999).

[19] A. Gavron, Phys. Rev. C21, 230 (1980).

[20] K. Hagino, N. Rowley, and A. T. Kruppa, Comput. Phys. Commun. 123, 143 (1999).

[21] C. H. Dasso, S. Landowne, and A. Winther, Nucl. Phys. A405, 381 (1983), Nucl. Phys. A407, 221 (1983).

[22] S. Landowne, S.C. Pieper, Phys. Rev. C 29 (1984) 1352.

[23] P. Ring, H. Massmann, J.O. Rasmussen, Nucl. Phys. A 296 (1978) 50

[24] M.A. Melkanoff, T. Sawada, J. Raynal, Meth. Comput. Phys. 6 (1966) 1.

[25] M.W. Kermode, N. Rowley, Phys. Rev. C 48 (1993) 2326.

[26] K. Hagino, N. Takigawa, M. Dasgupta, D.J. Hinde, J.R. Leigh, Phys. Rev. C 55 (1997) 276.

[27] G.F. Bertsch, P.F. Bortignon, K. Hagino, Nucl. Phys. A, in press.

[28] C.H. Dasso, G. Pollarolo, Phys. Lett. B 155 (1985) 223; C.H. Dasso, A. Vitturi, Phys. Lett. B 179 (1986) 337.

[29] J. L. Dethier and F. L. Stancu, Phys. Rev. C 23 (1981) 1503.

[30] L. C. Vaz and J. M. Alexander, Phys. Rev. C 18 (1978) 2152.

[31] D. Galetti and M. A. C. Ribeiro, Phys. Rev. C 50 (1994) 2136.

[32] M. Beckerman, Rep. Prog. Phys. 51 (1988) 1047.

[33] M. Dasgupta et al., Annu. Rev. Nucl. Part. Sci. 48 (1998) 401.

[34] L. F. Canto et al., Phys. Rep. 424 (2006) 1.

[35] R. G. Stokstad and E. E. Gross, Phys. Rev. C 23 (1981) 281.

[36] M. Dasgupta *et. al*., Annu. Rev. Nuc. Part. Sci. 48, 401 (1998).

[37] J. O. Newton *et al*., Phys. Lett. B 586 (2004) 219.

[38] K. Hagino *et al*., Phys. Rev. C 71 (2005) 044612.

[39] K. Hagino *et al*., Phys. Rev. C 67 (2003) 054603.

[40] K. Hagino and Y. Watanabe, Phys. Rev. C 76 (2007) 021601(R).

[41] M. Dasgupta *et al*., Prog. Theor. Phys. Suppl. 154 (2004) 209.

[42] K. Hagino and N. Takigawa, Prog. Theor. Phys. 128 (2012) 1061.

[43] N. Takigawa and K. Hagino, Prog. Theor. Phys. Suppl. 124 (1996) 101.

Plagiarism Report

URKUND

Document Information

Analyzed document	Hitakshi Thesis.docx (D76247926)
Submitted	7/11/2020 3:19:00 AM
Submitted by	
Submitter email	dheeraj.kumar@thapar.edu
Similarity	7%
Analysis address	dheeraj.kumar.thapar@analysis.urkund.com

Sources included in the report

SA	**Dissertation.pdf** Document Dissertation.pdf (D34283297)	1
SA	**Thesis.pdf** Document Thesis.pdf (D21248235)	1
J	**Subbarrier Fusion Reactions and Many-Particle Quantum Tunneling** URL: aeb44edc-ac98-4113-b4c2-807017286ffb Fetched: 3/4/2019 7:24:18 PM	2
SA	**Arts and Science-2019 -final.docx** Document Arts and Science-2019 -final.docx (D61414699)	1
W	URL: https://s3.cern.ch/inspire-prod-files-f/fc56ae915130a16f8b5cfdbd7998def7 Fetched: 5/29/2020 7:07:22 PM	2
SA	**Analysis of fusion.pdf** Document Analysis of fusion.pdf (D38758234)	1
W	URL: https://www.redalyc.org/pdf/464/46444888001.pdf Fetched: 10/15/2019 11:16:53 AM	2
W	URL: https://www.researchgate.net/publication/243570450_The_Nuclear_Potential_in_Heavy- ... Fetched: 12/24/2019 9:53:56 AM	6
W	URL: https://www.researchgate.net/publication/225608572_Interaction_and_Fusion_of_Defor ... Fetched: 7/11/2020 3:21:00 AM	3
W	URL: https://arxiv.org/pdf/nucl-th/0506073 Fetched: 7/11/2020 3:21:00 AM	1
W	URL: https://www.researchgate.net/publication/320979952_The_role_of_the_breakup_channel ... Fetched: 7/11/2020 3:21:00 AM	1
SA	**Investigation of interaction ... etc.pdf** Document Investigation of interaction ... etc.pdf (D34744497)	2

1/26